Supplementary information

S.1. Physical characterization of rGO-CM synthesized with different curcumin concentrations

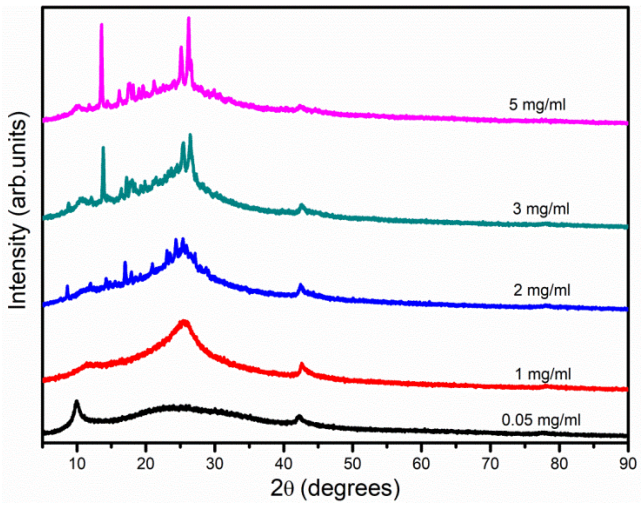

Figure S1: XRD patterns of rGO-CM synthesized with different curcumin concentrations

From Figure S1, it is observed that all the samples exhibit the peak corresponding to rGO. For low curcumin loading (0.05 and 1 mg/ml), the GO peaks also coexist with rGO, indicating partial reduction. In addition to the graphitic peaks, the peaks of curcumin are observed in the rest of the samples, indicating composite formation. The curcumin peak intensity increases with increasing loading. The GO peaks are suppressed in these samples, suggesting that most of the GO has been converted to rGO.

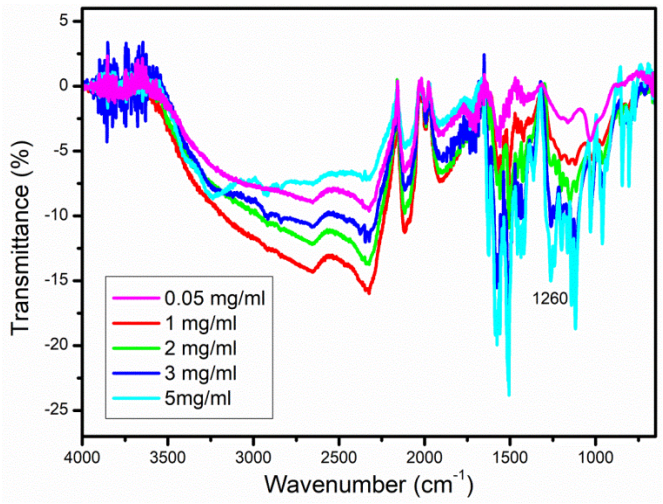

Figure S2: FTIR spectra of rGO-CM samples synthesized with different curcumin concentrations

The 1260 cm^{-1} peak, which corresponds to the C-O methyl bond of curcumin, increases with increasing curcumin concentration. The vibrations related to oxygen-containing groups are found to decrease with increasing curcumin, confirming the reduction of GO by curcumin.

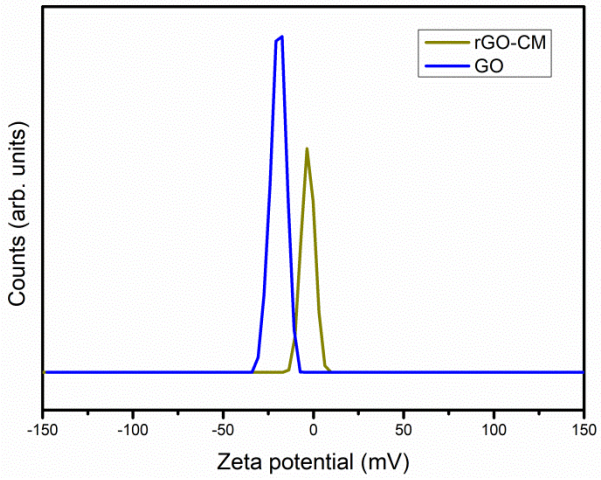

Figure S3: Zeta potential distributions of GO and rGO-CM

S.2.: Electrochemical characterization of rGO-CM synthesized with different curcumin concentrations

In order to compare the sensing performances of the different rGO-CMs, they were coated on glassy carbon electrodes, as mentioned previously. The electrochemical impedance of the rGO-CM/GCEs was measured in a 1:1 mixture of 0.018 M PBS buffer and $K_3[Fe(CN)_6]/K_4[Fe(CN)_6]$ (1:1) in a frequency range of 0.01 – 10^5 Hz. The corresponding Nyquist plots are depicted in Figure S3. It can be observed that the lowest R_{ct} is observed for rGO-CM-2 mg/ml, implying better electron transfer.

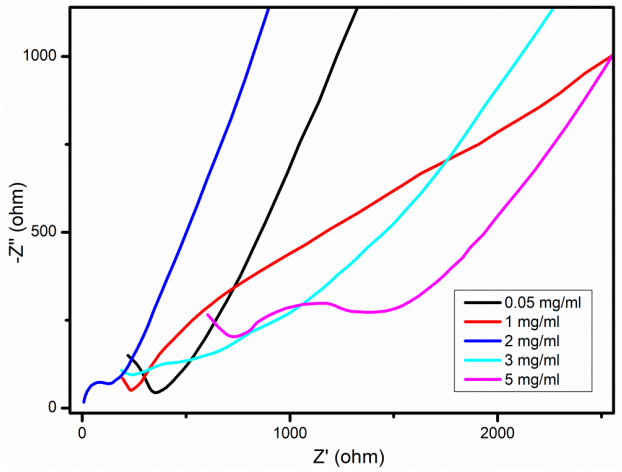

Figure S4: Nyquist plots of rGO-CM (synthesized with different curcumin concentrations) modified electrodes

Further, the current response of the rGO-CM/GCEs in 15 mM dioxane was studied. The LSVs observed are depicted in Figure S4. It was observed that the highest current at +1.5 V in response to 15 mM dioxane was exhibited by rGO-CM-2 mg/ml. These results indicate that 2 mg/ml concentration may be optimum for curcumin. For lower concentrations, the reduction is incomplete, implying the presence of lower conductivity graphite oxide, which decreases the current response. At higher curcumin concentrations, curcumin with low conductivity dominates the material.

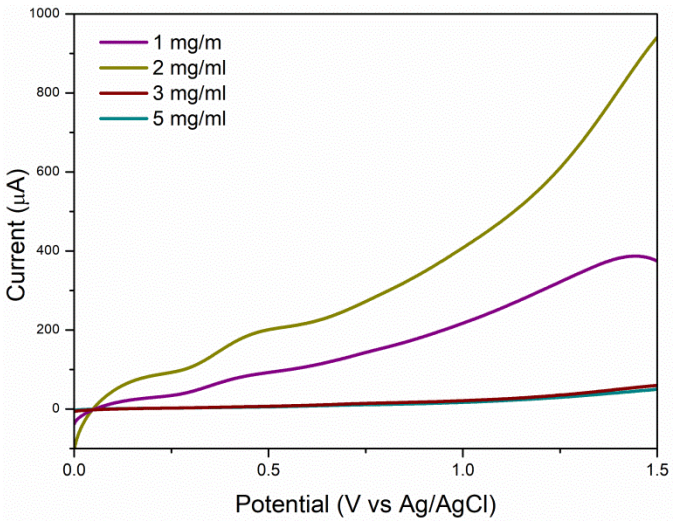

Figure S5: Linear sweep voltammograms of rGO-CM (synthesized with different curcumin concentrations) modified glassy carbon electrode in 15 mM dioxane.

S.3: Investigation of the oxidation product

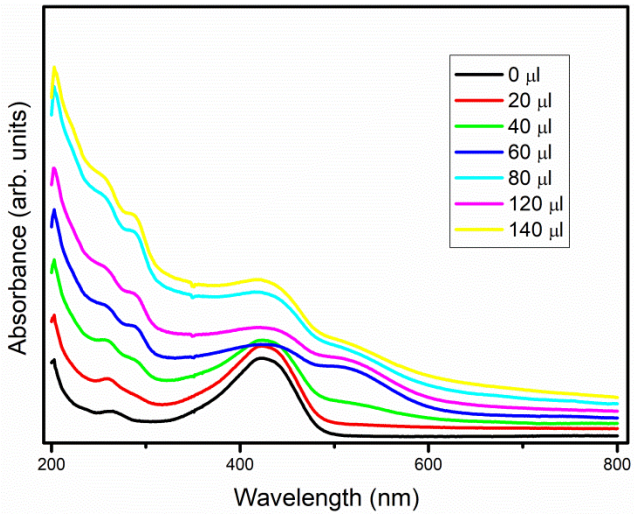

Figure S6: UV-Vis spectra of rGO-CM solution with serial addition of 1,4-dioxane

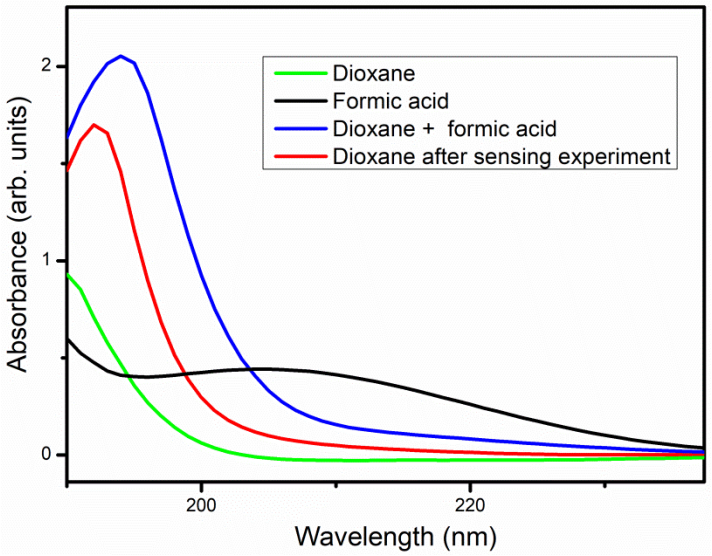

Figure S7: UV-Vis spectroscopy for the identification of the oxidation products

S.4: Analysis of sensing parameters of the rGO-CM/GCE

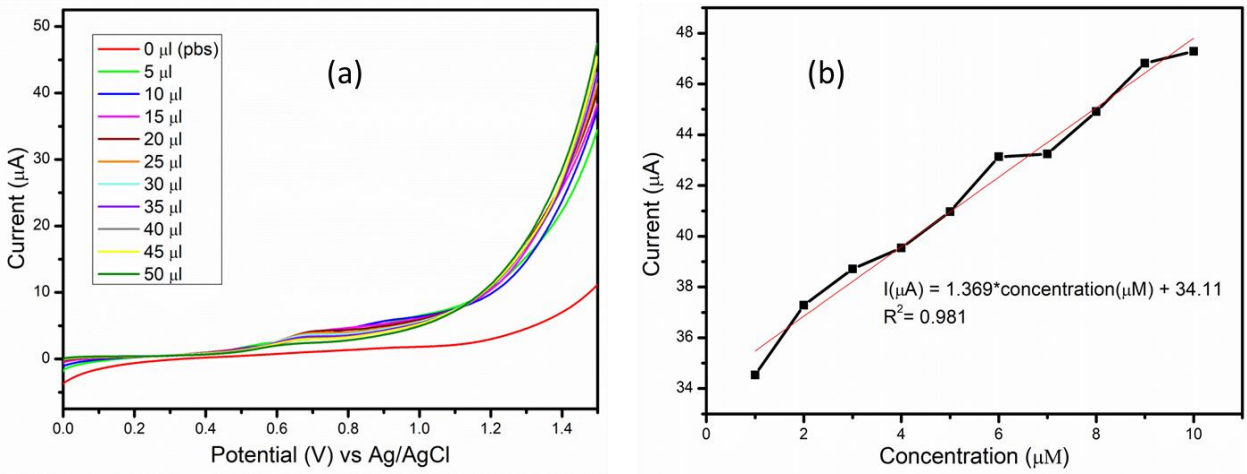

Figure S8: (a) Linear sweep voltammograms of rGO-CM/GCE in increasing concentration (1-10 µM) of 1,4-dioxane and (b) the corresponding calibration curve with the red line indicating the best linear fit.

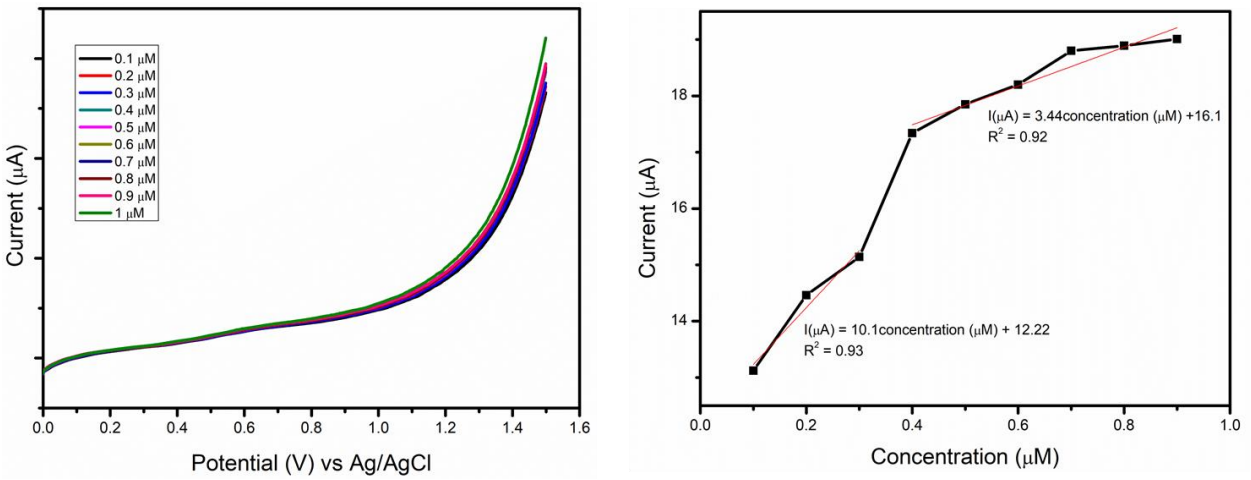

Figure S9: (a) Linear sweep voltammograms of rGO-CM/GCE in increasing concentration (0.1-1 μM) of 1,4-dioxane and (b) the corresponding calibration curve with the red line indicating the best linear fit.

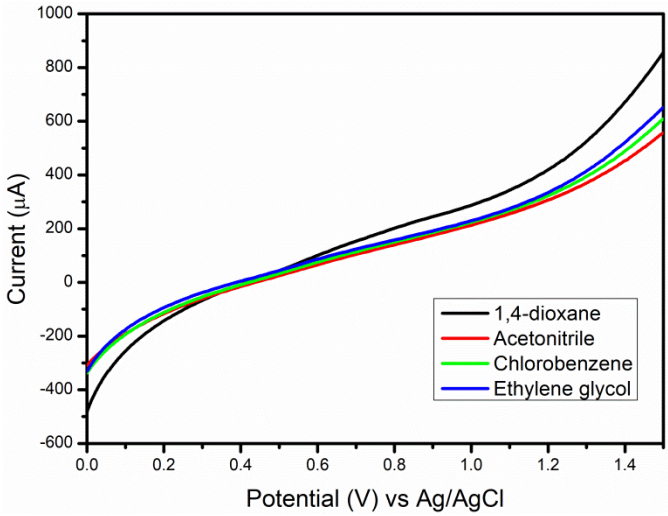

Figure S10: LSV of rGO-CM/GCE in dioxane and other interferants

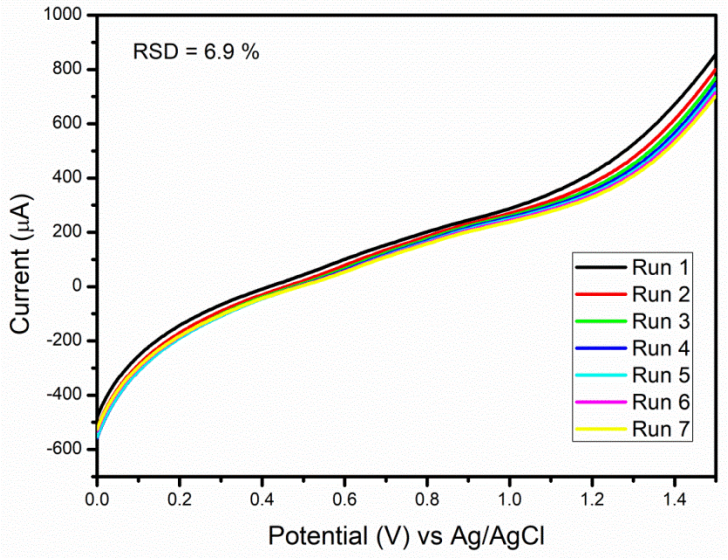

Figure S11: Stability of the current response of the rGO-CM/GCE sensor over seven consecutive runs

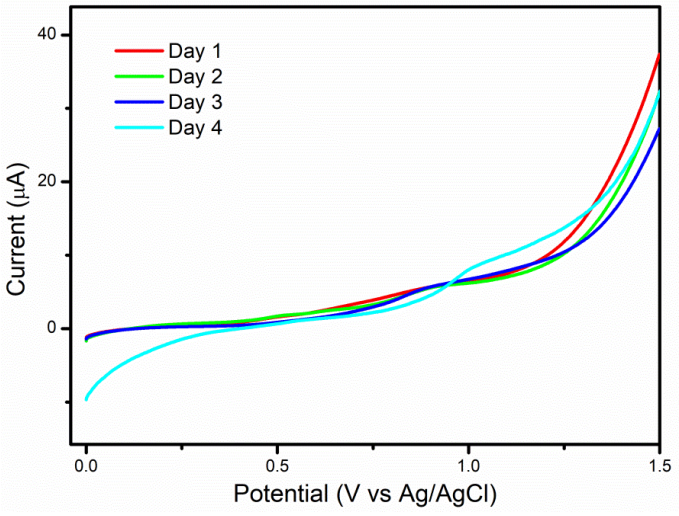

Figure S12: Stability of the rGO-CM/GCE sensor performance towards dioxane detection on different days

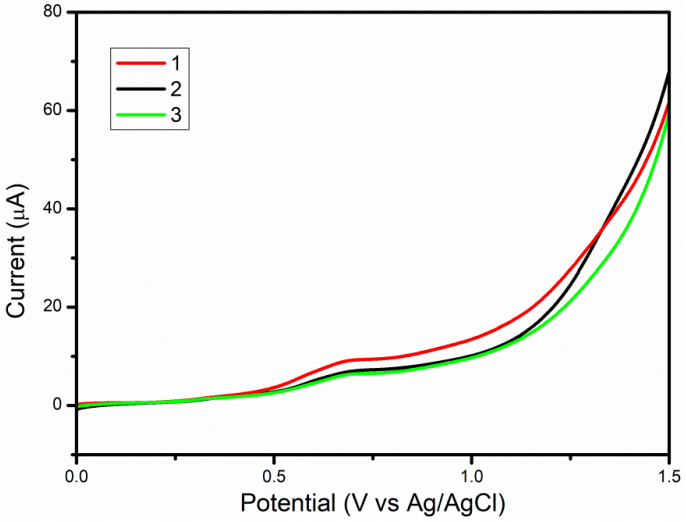

Figure S13: LSV of the rGO-CM coated on different GCEs

Table S1: Comparison of the analytical parameters of the sensors reported in literature versus the present work

Electrode	**Linear range**	**LOD**	**Sensitivity (µA µM^{-1} cm^{-2})**	**Reference**
PANI-SiO_2 NC	0.12 nM – 1.2 mM	16 pM	0.5934	[1]
NiO@Nd_2O_3 NC/GCE	0.12 nM – 0.12 mM	33 pM	0.029	[2]
ZnO/NiO/MnO_2/GCE	0.12 nM – 1.2 mM	9.14 pM	1.0417	[3]
rGO-CM/GCE	60 – 102 µM	0.13 µM	9.445	Present work
	6- 54 µM		4.67	
	1 – 10 µM		19.36	
	0.4 – 0.9 µM		48.65	
	0.1 - 0.3 µM		142.8	

1 M. R. Karim, M. M. Alam, M. O. Aijaz, A. M. Asiri, M. A. Dar and M. M. Rahman, *Talanta*, 2019, **193**, 64–69.

2 M. M. Rahman, A. Wahid and A. M. Asiri, *New J. Chem.*, 2019, **43**, 17395–17402.

3 M. M. Rahman, M. M. Alam and A. M. Asiri, *RSC Adv.*, 2019, **9**, 42050–42061.